Parametric Resonance in Quantum Field Theory

Jürgen Berges and Julien Serreau

Institute for Theoretical Physics, Heidelberg University, Philosophenweg 16, 69120 Heidelberg, Germany

(Received 8 August 2002; published 8 September 2003)

We present the first study of parametric resonance in quantum field theory from a complete next-to-leading order calculation in a $1/N$ expansion of the two-particle irreducible effective action, which includes scattering and memory effects. We present a complete numerical solution for an $O(N)$-symmetric scalar theory and provide an approximate analytic description of the nonlinear dynamics in the entire amplification range. We find that the classical resonant amplification at early times is followed by a collective amplification regime with explosive particle production in a broad momentum range, which is not accessible in a leading-order calculation.

DOI: 10.1103/PhysRevLett.91.111601 PACS numbers: 11.10.Wx, 11.15.Pg

In quantum field theory the phenomenon of parametric resonance describes the resonant amplification of quantum fluctuations, which can be interpreted as particle production. It provides an important building block for our understanding of the (pre)heating of the early universe after a period of inflation [1]. It has been frequently discussed for relativistic heavy-ion collisions in the formation of disoriented chiral condensates [2], or the decay of Polyakov-loop condensates [3], or parity-odd bubbles [4].

Despite being a basic phenomenon that can occur in a large variety of quantum field theories, parametric resonance is a rather complex process, which has so far defied most attempts for a complete analytic treatment even for simple theories. It is a far-from-equilibrium phenomenon involving densities inversely proportional to the coupling. The nonperturbatively large occupation numbers cannot be described by standard kinetic descriptions. So far, classical statistical field theory simulations on the lattice have been the only quantitative approach available [5]. These are valid for not too late times, before the approach to quantum thermal equilibrium sets in. Up to now, studies in quantum field theory have been mainly limited to linear or mean-field-type approximations (leading order in large N, Hartree) [6], which present a valid description for sufficiently early times. However, they are known to fail to describe thermalization and miss important rescattering effects [5,7]. Going beyond mean field has long been a major difficulty in practice: Similar to perturbation theory, standard approximations such as based on $1/N$ expansions of the one-particle irreducible (1PI) effective action can be secular in time and do not provide a valid description. In contrast, it has recently been demonstrated [8,9] for $1+1$ dimensional theories that far-from-equilibrium dynamics and subsequent thermalization can be described using a $1/N$ expansion of the *two-particle irreducible* (2PI) effective action [9–11]. Below, we show that this provides a systematic and *practicable* nonperturbative approach for quantum field theories in $3+1$ dimensions and with a nonzero macroscopic field ϕ, relevant for realistic particle physics applications.

In this work, we present the first quantum field theoretical description of the phenomenon of parametric resonance taking into account rescattering: For an $O(N)$-symmetric scalar field theory we employ the 2PI $1/N$ expansion to next-to-leading order (NLO), which includes off-shell and memory effects [9,11]. We point out that the approach solves the problem of an explicit description of the dynamics of correlation functions at nonperturbatively large densities. We present a complete numerical solution of the corresponding equations of motion. Moreover, we identify the relevant contributions to the dynamics at various times and provide an approximate analytic description of the nonlinear dynamics for the entire amplification range. Apart from the resonant amplification in the linear regime, we identify two characteristic time scales, which signal strongly enhanced particle production in a broad momentum range due to nonlinear, source effects. This collective amplification is crucial for the rapid approach to a subsequent, quasistationary regime, where direct scattering drives a very slow evolution towards thermal equilibrium. We emphasize that these processes cannot be seen in mean-field approximations. Similar phenomena have been observed in classical-field theories [5], and we present an analytic criterion for the validity of classical statistical approximations. These effects are important for a reliable description of the system at the end of the resonance stage for finite $N \lesssim 1/\lambda$. For realistic inflationary models with typically $\lambda \ll 1$ this is, in particular, crucial to determine whether there are any radiatively restored symmetries.

We consider a relativistic real scalar field φ_a ($a = 1, \ldots, N$) with action $S[\varphi] = -\int_x \{\frac{1}{2}\varphi_a(\Box_x + m^2)\varphi_a + (\lambda/4!N)(\varphi_a\varphi_a)^2\}$, where summation over repeated indices is implied. We use the notation $\int_x \equiv \int_C dx^0 \int d\mathbf{x}$ with C denoting a closed time path along the real axis. All correlation functions of the quantum theory can be obtained from the 2PI generating functional for Green's functions $\Gamma[\phi, G]$, parametrized by the field expectation value $\phi_a(x) = \langle\varphi_a(x)\rangle$ and the connected propagator $G_{ab}(x,y) = \langle \mathrm{T}_C \varphi_a(x)\varphi_b(y)\rangle - \phi_a(x)\phi_b(y)$ [10]:

 0031-9007/03/91(11)/111601(4)$20.00

$$\Gamma[\phi, G] = S[\phi] + \frac{i}{2}\mathrm{Tr}\ln G^{-1} + \frac{i}{2}\mathrm{Tr}G_0^{-1}(\phi)G + \Gamma_2[\phi, G],$$

where $iG^{-1}_{0,ab}(x, y; \phi) \equiv \delta^2 S[\phi]/\delta\phi_a(x)\delta\phi_b(y)$. The term $\Gamma_2[\phi, G]$ contains all contributions beyond one-loop order and can be represented as a sum over closed 2PI graphs [10]. To NLO in the 2PI $1/N$ expansion, $\Gamma_2[\phi, G]$ contains the diagrams with topology shown in Fig. 1 [9,11]. The infinite series can be summed analytically and the equations of motion [12] are obtained as

$$\frac{\delta\Gamma[\phi, G]}{\delta\phi_a(x)} = 0, \qquad \frac{\delta\Gamma[\phi, G]}{\delta G_{ab}(x, y)} = 0. \tag{1}$$

As we will show below, for the phenomenon of parametric resonance, each diagram of the infinite series in Fig. 1 eventually contributes at the same order in the coupling λ. In this sense, the 2PI $1/N$ expansion to NLO represents a minimal approach for a controlled description including rescattering. This justifies the rather involved complexity of the approximation.

Overview.—Parametric amplification of quantum fluctuations can be best studied in a weakly coupled system that is initially in a pure quantum state, characterized by a large "classical" field amplitude $\phi_a(t) = \sigma(t)M_0\sqrt{6N/\lambda}\,\delta_{a1}$, and small quantum fluctuations, corresponding to vanishing particle numbers at initial time. Here M_0 sets our unit of mass and the rescaled field $\sigma(t = 0) \equiv \sigma_0$ is of order unity. We first present results from a full numerical [13] integration of the time evolution at NLO. In Fig. 2 we show the classical field and the fluctuation contributions to the (conserved) total energy as functions of time. The former dominates at early times and one observes that more and more energy is converted into fluctuations as the system evolves. A characteristic time — denoted as t_{nonpert} in Fig. 2 — is reached when the classical and the fluctuation parts of the energy become of the same size. Before this time, the coherent oscillations of the field ϕ lead to a resonant enhancement of fluctuations in a narrow range of momenta around a specific value $|\mathbf{p}| \simeq p_0$: this is parametric resonance [1,6]. Nonlinear interactions between field modes then cause this amplification to spread to a broad range of momenta. We find that the resulting rate of amplification exceeds the characteristic rate γ_0 for the resonant growth. This is illustrated in Figs. 3 and 4, where the effective particle numbers [8] are displayed for various momenta as a function of time, both for the transverse ($G_\perp$) and the longitudinal ($G_\parallel$) sector, with $G_{ab} = \mathrm{diag}\{G_\parallel, G_\perp, \ldots, G_\perp\}$. One observes that, in contrast to the rapid changes for particle numbers before t_{nonpert}, a comparably slow quasistationary evolution takes place at later times. The fluctuation dominated regime for $t \gtrsim t_{\mathrm{nonpert}}$ is characterized by strong nonlinearities. For instance, from Fig. 2 one infers for $t \simeq t_{\mathrm{nonpert}}$ that the classical-field decay "overshoots" and is temporarily reversed by feedback from the modes. This can be directly seen in the evolution for the rescaled field shown in Fig. 5. The particle numbers of Figs. 3 and 4 exhibit correspondingly a reverse behavior. Very similar phenomena have been observed in related classical theories [5], though a direct comparison requires simulations for the same model as studied here [14]. There the full nonlinearities, i.e., including *all orders* in $1/N$, are taken into account while leaving out quantum corrections. This indicates the capability of the 2PI $1/N$ expansion at NLO to capture the dominant nonlinear dynamics.

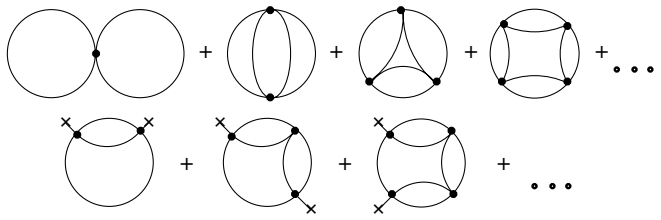

FIG. 1. The dots indicate that each diagram is obtained from the previous one by adding another "rung" with two full propagator lines at each vertex. The crosses denote field insertions.

The characteristic properties described above can be understood analytically from the evolution equations for the Fourier modes of the one- and two-point functions. Separating real and imaginary parts with $G_{\parallel,\perp}(t, t'; \mathbf{p}) = F_{\parallel,\perp}(t, t'; \mathbf{p}) - \frac{i}{2}\rho_{\parallel,\perp}(t, t'; \mathbf{p})\mathrm{sgn}_C(t - t')$, the real $\rho_{\parallel,\perp}$ denote the spectral and $F_{\parallel,\perp}$ the statistical two-point functions [8,9]. We define

$$M^2(t) = m^2 + \frac{\lambda}{6N}[3T_\parallel(t) + (N - 1)T_\perp(t)], \tag{2}$$

where $T_{\parallel,\perp}(t) = \int^\Lambda [d\mathbf{p}/(2\pi)^3]F_{\parallel,\perp}(t, t; \mathbf{p})$ with $\Lambda \gg p_0$. Initially, $F_\parallel(0, 0; \mathbf{p}) = 1/2\omega_\parallel(\mathbf{p})$, $\partial_t F_\parallel(t, 0; \mathbf{p})|_{t=0} = 0$, $\partial_t\partial_{t'}F_\parallel(t, t'; \mathbf{p})|_{t=t'=0} = \omega_\parallel(\mathbf{p})/2$, and similarly for $F_\perp$. The frequencies are $\omega_\parallel(\mathbf{p}) = [\mathbf{p}^2 + M_0^2(1 + 3\sigma_0^2)]^{1/2}$, $M_0^2 \equiv M^2(0)$, and similarly for $\omega_\perp(\mathbf{p})$ with $3\sigma_0^2 \to \sigma_0^2$. The initial conditions for the spectral functions are fixed by the equal-time commutation relations: $\rho_{\parallel,\perp}(t, t'; \mathbf{p})|_{t=t'} = 0$ and $\partial_t\rho_{\parallel,\perp}(t, t'; \mathbf{p})|_{t=t'} = 1$ [8,9].

(I) Early-time linear (Lamé) regime: parametric resonance.—At early times the σ-field evolution equation

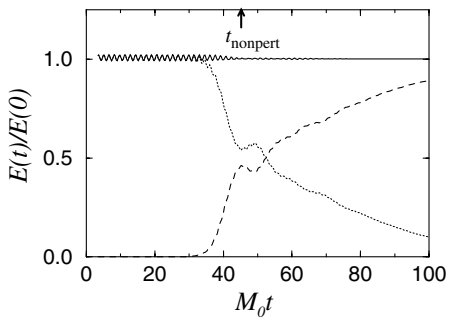

FIG. 2. Total energy (solid line) and classical-field energy (dotted line) as a function of time for $\lambda = 10^{-6}$. The dashed line represents the fluctuation part, showing a transition from a classical-field to a fluctuation dominated regime.

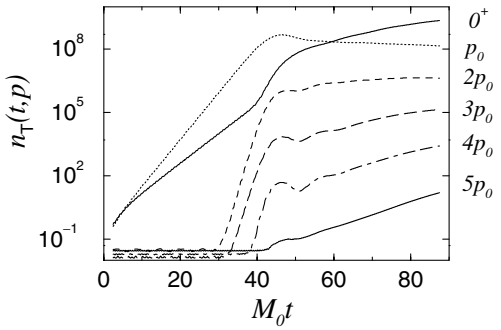

FIG. 3. Effective particle number density for the transverse modes as a function of time for various momenta $p \leq 5p_0$. At early times, modes with $p \simeq p_0$ are exponentially amplified with a rate $2\gamma_0$. Because of nonlinearities, one observes subsequently an enhanced growth with rate $6\gamma_0$ for a broad momentum range.

receives the dominant $[O(\lambda^0)]$ contributions from the classical action S. The classical-field dynamics is characterized by rapid oscillations with constant amplitude and period $2\pi/\omega_0$. The evolution equations for the two-point functions at $O(\lambda^0)$ correspond to free-field equations with the addition of a time dependent mass term $3\sigma^2(t)$ for the longitudinal and $\sigma^2(t)$ for the transverse modes. The dynamics in this linear regime has been extensively studied in the literature and is known to be described by the solution of a Lamé equation [1,6]: Parametric resonance manifests itself by an exponential growth of the statistical two-point functions describing particle production in a narrow momentum range with $p^2 \leq (\sigma_0^2/2)$. Averaging over the short-time scale $\sim\omega_0^{-1}$ one finds for the *transverse* modes for $t, t' \gg \gamma_0^{-1}$:

$$F_\perp(t, t'; \mathbf{p}_0) \sim e^{\gamma_0(t+t')}, \tag{3}$$

for the maximally enhanced mode with $p_0 \simeq (\sigma_0/2)$. One finds a much smaller growth for the *longitudinal* modes (cf. also Fig. 4). The analytic solution to $O(\lambda^0)$ agrees accurately with the NLO numerical results at early times.

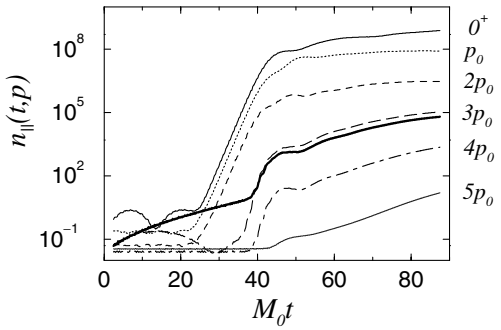

FIG. 4. Same as in Fig. 3, for the longitudinal modes. Nonlinear source effects trigger an exponential growth with rate $4\gamma_0$ for $p \lesssim 2p_0$. The thick line corresponds to a mode in the parametric resonance band, and the long-dashed line for a similar one outside the band. The resonant amplification is quickly dominated by source-induced particle production.

(II) Source-induced amplification regime: enhanced particle production for longitudinal modes.—Because of the exponential growth of the transverse fluctuations for $\gamma_0 t \gg 1$, the $O(\lambda^0)$ approximation eventually breaks down at some time. Using the two-loop graphs of Fig. 1, at $O(\lambda)$ the evolution equation for $F_\parallel$ can be approximated by

$$[\partial_t^2 + \mathbf{p}^2 + 3\sigma^2(t) + M^2(t)]F_\parallel(t, t'; \mathbf{p}) \simeq 2\alpha\sigma^2(t)T_\perp(t)F_\parallel(t, t'; \mathbf{p}) + \alpha\sigma(t)\sigma(t')\Pi_\perp^F(t, t'; \mathbf{p}), \tag{4}$$

with $\Pi_\perp^F(t, t'; \mathbf{p}) = \int d\mathbf{q} F_\perp(t, t'; \mathbf{p} - \mathbf{q})F_\perp(t, t'; \mathbf{q})$, and $\alpha = \lambda/(2\pi)^3(N - 1/6N)(c^2/\omega_0^2)$ with constant $c \sim 1$. Here, we have used that the momentum integrals are dominated by the amplified transverse modes. In addition, we exploit the fact that, for $t'' \simeq t \lesssim t_{\text{nonpert}}$,

$$F_\perp^2(t, t''; \mathbf{p}_0) \gg \rho_\perp^2(t, t''; \mathbf{p}_0)/4. \tag{5}$$

Its validity can be seen from (3) and the corresponding behavior of $\rho_\perp(t, t''; \mathbf{p}_0) \sim e^{\gamma_0(t-t'')}$ for $t'' \lesssim t$. We emphasize that strictly neglecting in the evolution equations ρ^2 terms as compared to F^2 terms for *all* modes and *all* times corresponds to the classical statistical field theory limit [9]. This provides an explicit analytic criterion for the applicability of the classical methods employed in [5]. For sufficiently early times, all momentum integrals are indeed dominated by the enhanced modes $\mathbf{p} \simeq \mathbf{p}_0$ for which (5) is valid. A detailed analysis reveals that the memory integrals appearing in the equations of motion are dominated by the latest times $t'' \simeq t$: One can explicitly verify that effective locality, described by the replacement $\int_0^t dt'' \to \int_{t-c/\omega_0}^t dt''$ [cf. Eq. (4)], is valid for the time-averaged behavior over the short-time scale $\sim\omega_0^{-1}$. We conclude that classical statistical approximations can provide a good description in this regime.

The first term on the right-hand side of (4) is a NLO contribution to the mass, whereas the second term represents a source term, resulting from annihilations of amplified transverse modes as well as stimulated emission processes. To evaluate the momentum integrals, we use a saddle point approximation around

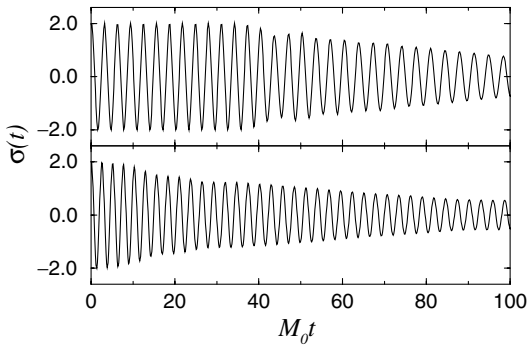

FIG. 5. The rescaled field σ as a function of time for $\lambda = 10^{-6}$ (top panel) and $\lambda = 10$ (bottom panel).

$p \simeq p_0$, valid for $t, t' \gg \gamma_0^{-1}$, with $F_\perp(t, t', \mathbf{p}) \simeq F_\perp(t, t', \mathbf{p}_0) \exp[-|\gamma_0''|(t + t')(p - p_0)^2/2]$:

$$T_\perp(t) \simeq \frac{p_0^2 F_\perp(t, t; \mathbf{p}_0)}{2(\pi^3 |\gamma_0''| t)^{1/2}}, \tag{6}$$

$$\Pi_\perp^F(t, t'; 0) \simeq \frac{p_0^2 F_\perp^2(t, t'; \mathbf{p}_0)}{4[\pi^3 |\gamma_0''|(t + t')]^{1/2}}. \tag{7}$$

Here we wrote the source term for its maximum at $\mathbf{p} = 0$. More precisely, it affects all modes with $\mathbf{p} \lesssim 2\mathbf{p}_0$. An important characteristic time is reached when the mass corrections become comparable to the classical mass term. This can be seen to happen at $t_{\text{nonpert}} \simeq (\ln\lambda^{-1})/(2\gamma_0)$, when $T_\perp \simeq O(\lambda^{-1})$ (see also [6]). Note that at this time, both the LO and the NLO mass terms are of the *same* order in λ, but with opposite sign. We point out that the source term in (4) becomes important at the *earlier* time

$$t_{\text{source}} \simeq t_{\text{nonpert}}/2, \tag{8}$$

when $F_\perp(t, t'; \mathbf{p}_0) \simeq O(N^0 \lambda^{-1/2})$. For $t \gtrsim t_{\text{source}}$, the exponentially growing source drives the dynamics of longitudinal modes and one finds a strong amplification for $p \lesssim 2p_0$: $F_\parallel(t, t'; \mathbf{p}) \sim \exp[2\gamma_0(t + t')]$. This agrees precisely with the numerical results shown in Fig. 4.

(III) Collective amplification regime: explosive particle production in a broad momentum range.—A similar analysis can be made for the transverse fluctuations. The approximate evolution equation for $F_\perp$ has a similar structure as (4). Beyond the $O(\lambda^0)$ (Lamé) description, it receives contributions from the feedback of the longitudinal modes at $O(\lambda)$ and from the amplified transverse mode at $O(\lambda^2)$. The corresponding mass corrections remain small until t_{nonpert}, whereas the source term is parametrically of the form $\sim\lambda^2 F_\perp^3/N$. This leads to the characteristic time

$$t_{\text{collect}} \simeq 2t_{\text{nonpert}}/3 + (\ln N)/(6\gamma_0) \tag{9}$$

at which $F_\perp(t, t'; \mathbf{p}_0) \simeq O(N^{1/3}\lambda^{-2/3})$. Correspondingly, for $t_{\text{collect}} \lesssim t \lesssim t_{\text{nonpert}}$ one finds a large particle production rate $\sim 6\gamma_0$ for a wide range of momenta, in agreement with the full NLO results in Fig. 3. In this time range the longitudinal modes exhibit an enhanced amplification as well (cf. Fig. 4). The abundant particle production is accompanied by an exponential decrease of the classical-field energy. We emphasize that the collective amplification regime is absent in the LO large-N approximation. Consequently, even for the transverse sector the latter does not give an accurate description at intermediate times if $t_{\text{collect}} \lesssim t_{\text{nonpert}}$, that is for $N \lesssim \lambda^{-1}$.

(IV) Nonperturbative regime: quasistationary evolution.—At $t \simeq t_{\text{nonpert}}$ one finds $F_\perp(t, t'; \mathbf{p}_0) \simeq O(N^0\lambda^{-1})$. As a consequence, there are leading contributions ($\sim \lambda^0$) to the dynamics coming from all loop orders (cf. Fig. 1). In particular, the evolution equations are no longer "local" in the sense described under (II) and memory effects become important. In contrast to the rapid resonant dynamics before t_{nonpert}, a comparably slow, quasistationary evolution driven by direct scattering sets in. We emphasize that the collective amplification regime triggered a rapid approach to monotonously decreasing particle number distributions as functions of momentum, which become quasistationary afterwards (cf. Figs. 3 and 4). The approach to true thermal equilibrium is exceedingly slow for the employed range of couplings $\lambda = 10^{-6}$–10, for which a non-negligible parametric resonance regime can be observed. For phenomenological applications it is therefore crucial that in the quasistationary, prethermal regime in the spirit of Refs. [2,14] a number of aspects do not differ much from the late-time thermal regime [15].

We thank R. Baier, C. Wetterich, and T. Prokopec for fruitful discussions. Numerical computations were done on the PC cluster HELICS of the Interdisciplinary Center for Scientific Computing (IWR), Heidelberg University.

[1] J. H. Traschen and R. H. Brandenberger, Phys. Rev. D **42**, 2491 (1990); L. Kofman, A. D. Linde, and A. A. Starobinsky, Phys. Rev. Lett. **73**, 3195 (1994).
[2] S. Mrówczyński and B. Müller, Phys. Lett. B **363**, 1 (1995).
[3] A. Dumitru and R. D. Pisarski, Phys. Lett. B **504**, 282 (2001).
[4] D. Ahrensmeier, R. Baier, and M. Dirks, Phys. Lett. B **484**, 58 (2000).
[5] S. Yu. Khlebnikov and I. I. Tkachev, Phys. Rev. Lett. **77**, 219 (1996); T. Prokopec and T. G. Roos, Phys. Rev. D **55**, 3768 (1997); I. Tkachev, S. Khlebnikov, L. Kofman, and A. D. Linde, Phys. Lett. B **440**, 262 (1998).
[6] D. Boyanovsky, H. J. de Vega, R. Holman, and J. F. J. Salgado, Phys. Rev. D **54**, 7570 (1996). One has $p_0 \simeq \sigma_0(1 - \delta)/2$, $\omega_0 \simeq 2\sqrt{1 + \sigma_0^2}(1 - 4\delta)$, $\gamma_0 \simeq 2\delta\omega_0$, $\gamma_0'' \simeq -64\gamma_0 p_0^2/\sigma_0^4$, with $\delta \leq e^{-\pi}$. For $\sigma_0 = 2$ used here, $\delta \simeq 3.2 \times 10^{-2}$.
[7] L. Kofman, A. D. Linde, and A. A. Starobinsky, Phys. Rev. D **56**, 3258 (1997).
[8] J. Berges and J. Cox, Phys. Lett. B **517**, 369 (2001); G. Aarts and J. Berges, Phys. Rev. D **64**, 105010 (2001).
[9] J. Berges, Nucl. Phys. **A699**, 847 (2002); G. Aarts and J. Berges, Phys. Rev. Lett. **88**, 041603 (2002).
[10] J. M. Cornwall, R. Jackiw, and E. Tomboulis, Phys. Rev. D **10**, 2428 (1974).
[11] G. Aarts, D. Ahrensmeier, R. Baier, J. Berges, and J. Serreau, Phys. Rev. D **66**, 045008 (2002).
[12] For details see Eqs. (5.1) and (B.6)–(B.14) of Ref. [11].
[13] Typical volumes $(N_s a_s)^3$ of $N_s = 36$–48 with $a_s = 0.4$–0.3 lead to results which are rather insensitive to finite-size and cutoff effects. Displayed numerical results are for $N = 4$. For details about the numerical method see [9].
[14] G. F. Bonini and C. Wetterich, Phys. Rev. D **60**, 105026 (1999).
[15] J. Berges, J. Serreau, and C. Wetterich (to be published).